Research Square

Preprints are preliminary reports that have not undergone peer review.
They should not be considered conclusive, used to inform clinical practice,
or referenced by the media as validated information.

Targeted delivery of therapeutic retroviral replicating vectors to glioma using adipose-derived stem cells

Shin-Wei Liao
National Chung Cheng University
Yi-Ting Chiu
National Chung Cheng University
Jui-Ming Sun
Ditmanson Medical Foundation Chia-Yi Christian Hospital
Pi-Chan Ko
Ditmanson Medical Foundation Chia-Yi Christian Hospital
Yu-Hao Chen
Ditmanson Medical Foundation Chia-Yi Christian Hospital
Chien-Kuo Tai
biockt@ccu.edu.tw

National Chung Cheng University

Research Article

Keywords: gene therapy, glioma, stem cells, retrovirus, prodrug activator

Posted Date: November 16th, 2026

DOI: https://doi.org/10.21203/rs.3.rs-11557030/v1

License: This work is licensed under a Creative Commons Attribution 4.0 International License.
Read Full License

Additional Declarations: No competing interests reported.

Targeted delivery of therapeutic retroviral replicating vectors to glioma using adipose-derived stem cells

Shin-Wei Liao[1], Yi-Ting Chiu[1], Jui-Ming Sun[2], Pi-Chan Ko[2], Yu-Hao Chen[2,3,*] and Chien-Kuo Tai[1,*]

[1]Department of Biomedical Sciences, National Chung Cheng University, Chia-Yi, Taiwan.

[2]Section of Neurosurgery, Department of Surgery, Ditmanson Medical Foundation Chia-Yi Christian Hospital, Chia-Yi, Taiwan.

[3]Center for General Education, Chia Nan University of Pharmacy and Science, Tainan, Taiwan.

[*]Correspondence email: 07454@cych.org.tw; biockt@ccu.edu.tw

ABSTRACT

Gene delivery using retroviral replicating vectors (RRVs) is highly efficient, with nearly full transduction occurring throughout tumors in small-animal glioma models. However, vector spread is still restricted by the dosage that can be delivered by a single injection of viral vector supernatant, particularly in the large and diffusely infiltrating tumors that are characteristic of human high-grade gliomas. This study attempted to further improve the efficacy of this approach by engineering adult human adipose-derived stem cells (hASCs) to function as the carrier and producer cells for RRVs. We investigated the capability of RRV-producing hASCs (hASC-RRVs) to yield RRVs and deliver the vector to gliomas. The results show that RRVs released from hASC-RRVs can efficiently infect glioma cells, achieving tumor-selective and persistent gene delivery to gliomas. We have also confirmed the tumor-tropic migratory ability of hASC-RRVs, which greatly improved the efficiency of RRV delivery *in vivo*. In addition, the therapeutic effect of RRVs delivered by hASCs was increased markedly. In an orthotopic mouse model of human glioma, after a single injection of hASC-RRVs, hASC-RRV-mediated prodrug activator gene therapy resulted in chronic suppression of tumor growth and prolonged survival of the animals. Thus, using hASCs as the carrier and producer for RRVs may represent a promising strategy for glioma gene therapy.

Keywords: gene therapy, glioma, stem cells, retrovirus, prodrug activator

INTRODUCTION

Glioma is the most common form of primary brain tumor, and is classified by the World Health Organization into four histopathological grades. Grade IV malignant glioma, also known as glioblastoma multiforme (GBM), is particularly aggressive and exhibits a universally poor prognosis [1]. This is largely due to the infiltrative nature of GBM cells, which spread into surrounding brain tissue and render localized therapies such as surgery and radiation largely ineffective [2]. Tumor recurrence remains almost inevitable even after applying standard treatment protocols, including maximal surgical resection followed by chemoradiotherapy, resulting in a median survival time of ~14 months for GBM patients [3].

The unmet need for effective treatment options has prompted investigations of new strategies such as gene therapy. However, no improvement in patient survival was achieved in clinical trials of GBM gene therapy using a standard (non-replicating) retroviral vector encoding herpes simplex virus thymidine kinase (HSV-TK) with subsequent administration of the prodrug ganciclovir, which was attributed to ineffective tumor transduction of the vector [4]. Transduction might be more efficient when using retroviral replicating vectors (RRVs), since the viral vector would replicate after the initial infection and each infected tumor cell would in effect become a viral vector producer cell, resulting in the progressive spread of the viral vector [5, 6]. We and others have previously demonstrated that murine leukemia virus (MLV)-based RRVs can achieve highly efficient, tumor-selective gene transfer to gliomas, resulting in the suppression of tumor growth and prolonged survival in immune-competent intracerebral glioma models. [7-9]. Furthermore, a phase 1 clinical trial (NCT01470794) of RRV-mediated prodrug activator gene therapy demonstrated survival improvement for patients with recurrent high-grade glioma [10]. The safety investigations in a randomized, open-label phase 2/3 trial (NCT02414165) demonstrated the safety profile of RRVs, although there were no additional survival benefits over standard treatment [11].

Despite the demonstrated efficacy of RRVs, their spread remains restricted by the dosage that can be delivered via a single injection of viral vector supernatant [9]. Although such an injected dose of RRVs will eventually spread to almost all of the actively dividing GBM cells, the distribution dynamics mean that there will be a significant lag time before viral replication can accelerate into the logarithmic spread

phase.

To further improve the efficacy of this novel therapeutic strategy, we aimed to exploit the tumor-homing ability of mesenchymal stem cells (MSCs) by engineering them to function as RRV producer cells. Previous studies have shown that the inflammatory chemokines and growth factors present in the tumor microenvironment can attract various types of MSC, including bone-marrow-derived MSCs and adipose-derived stem cells [12-15], which have led to them being investigated as potential tools for cancer therapy. The MSCs engineered to express therapeutic molecules such as IFN-α, IFN-β, IL-12, and TRAIL as well as prodrug activator enzymes such as HSV-TK and cytosine deaminase (CD) have demonstrated promising antitumor effects in preclinical models [16-25]. Notably, a clinical trial using genetically modified human adipose-derived stem cells (hASCs) for recurrent GBM has provided early evidence for the safety and feasibility of MSC-mediated gene therapy [26]. In contrast with bone marrow, human adipose tissue is easily accessed via minimally invasive procedures and can yield a significant number of hASCs [27-29]. Furthermore, hASCs are known for their immunomodulatory properties and low immunogenicity, allowing for potential allogeneic transplantation without eliciting significant immune responses [30]. Importantly, hASCs have been shown to exhibit glioma tropism and can effectively function as tumor-targeting carriers in experimental glioma models [31-34].

In this study we investigated the safety and feasibility of using hASCs as a delivery vehicle for RRVs encoding the yeast CD gene for glioma gene therapy. We first examined whether hASCs exhibit tumor-tropic behavior and are capable of delivering RRVs to glioma cells. We then evaluated the therapeutic efficacy of this delivery system in an orthotopic glioma model by monitoring tumor progression and survival following the intracerebral injection of hASCs and the systemic administration of the prodrug 5-fluorocytosine (5-FC), which was subsequently converted into a highly toxic metabolite 5-fluorouracil (5-FU) by CD. The obtained results indicate that hASCs can increase the efficacy and durability of RRV-mediated gene therapy, and thereby represent a promising strategy for targeted glioma treatment.

MATERIALS AND METHODS

Cell lines

The transformed human embryonic kidney cell line 293T and human glioma cell line U87 were grown in high-glucose DMEM (Thermo) supplemented with 10% fetal bovine serum (FBS, Invitrogen). hASCs (kindly provided by Dr S-M Huang, National Defense Medical Center, Taipei, Taiwan) were grown in low-glucose DMEM (Thermo) with 10% FBS [35]. The human astrocyte cell line SVGA was grown in MEM (Thermo) with Earle's balanced salts, 1 mM sodium pyruvate, 1 mM nonessential amino acid and 10% FBS.

Viral vector production and infection of hASCs

As described previously [36], plasmids pACE-GFP and pACE-CD encode replication-competent amphotropic MLV vectors, in which internal ribosome entry site (IRES)-GFP and IRES-CD gene cassettes, respectively, have been inserted between amphotropic *env* and 3′-untranslated region (3′-UTR). Viral vectors were produced by transient transfection of 293T cells with pACE-GFP or pACE-CD using Lipofectamine 2000 reagent (Invitrogen). For titer determination, viral supernatant was added to U87 cells at ~20% confluence in the presence of 4 μg/mL Polybrene (Sigma). Viral supernatant was removed at 24 h postinfection, and the cells were then incubated in regular media containing 50 μM 3′-azido-3′-deoxythymidine (AZT) (Sigma) for 48 h and analyzed for GFP expression using a flow cytometer (Becton Dickinson). Virus titers were quantified in transducing units (TU) per milliliter. For *in vitro* infection experiments, hASCs were infected with ACE-GFP at a multiplicity of infection (MOI) of 0.2 in the presence of 4 μg/mL Polybrene. Flow cytometry was used to analyze GFP expression by the cells at various time points postinfection, in order to ensure that the entire cell population exhibited fluorescence. Infection of ACE-CD to hASCs was performed in parallel until full transduction was achieved. The hASCs fully transduced with ACE-GFP and ACE-CD were designated as hASC-ACE-GFPs and hASC-ACE-CDs, respectively.

Viral vector replication assays in U87 glioma cells

Conditioned media collected from the hASC-ACE-GFP culture was diluted twofold and used to infect U87 cells. Flow cytometry was used to analyze GFP expression by

the cells at various time points postinfection. In a separate experiment, hASC-ACE-GFPs were mixed with U87-dsRed cells at 0.01%, 0.1%, and 1% of the cell population and seeded onto six-well plates. The expression levels of GFP and dsRed by the cell populations were analyzed at various time points postinfection.

Transwell cell migration assay

A cell migration assay was performed using 24-well Transwell plates with 8-μm-pore filter (Corning). U87 or SVGA (5×10^4 cells) were seeded onto the lower well of the Transwell plate and cultured overnight, after which the culture medium was replaced with DMEM supplemented with 0.5% FBS. In the upper well, 2×10^4 hASCs were seeded in DMEM supplemented with 0.5% FBS, and the cells were allowed to migrate for 36 h at 37°C. Non-migrated cells were removed from the apical side of the upper well, and the migrated cells were stained with Giemsa solution and their migration was quantified by counting cells in five high-power fields (×200) under a light microscope.

***In vitro* cytotoxicity assay**

hASCs, hASC-ACE-GFPs, and hASC-ACE-CDs were mixed with U87 cells at 10% of the cell population and seeded onto replicate 96-well plates at 3000 cells/well. After overnight culture, the mixed cell populations were exposed to 0.5 mM 5-FC (Sigma), and cell viability was determined 4 and 8 days later using the MTS assay with the CellTiter Aqueous One Solution Cell Proliferation Assay kit (Promega). In a separate experiment, hASC-ACE-CDs were seeded onto replicate 96-well plates at 3000 cells/well, and after overnight culture the cells were exposed to 0.5 mM 5-FC. The cell viability was determined every 4 days using the MTS assay.

Viral vector replication assay in intracerebral gliomas

All animal studies were performed in accordance with the institutional guidelines under protocol #1070201 (March 20, 2018) approved by the Institutional Animal Care and Use Committee at National Chung Cheng University. Intracerebral U87 gliomas were established by the stereotactic injection of 2×10^5 U87-dsRed cells into the right frontal lobe of BALB/c nude mice (National Laboratory Animal Center, Taipei, Taiwan) at 1 mm anterior and 1.5 mm lateral relative to the bregma, and 2.8 mm deep

in the brain. Five days later, the mice were stereotactically injected with 2×10^5 hASC-ACE-GFPs at the tumor implantation site or at the opposite left frontal lobe. The mice were sacrificed 4 weeks later, and tumors were excised and digested with collagenase (Invitrogen). The dissociated cells were filtered through 100-μm cell strainers, pelleted by centrifugation, resuspended in culture medium containing 50 μM AZT, and plated onto culture plates. After overnight culture, the cells were trypsinized and immediately subjected to flow cytometry to determine the expression levels of GFP and dsRed.

Fluorescence molecular tomography (FMT) imaging

A U87 cell line stably expressing near-infrared fluorescent protein (iRFP), U87-iRFP [37], was used to establish intracerebral glioma as described above. The FMT 4000 system (PerkinElmer) was used to detect iRFP fluorescence signals in mice weekly as described previously [37, 38]. In brief, each anesthetized mouse was placed in an imaging cassette in the prone position and taken into the FMT imaging chamber via a docking system. 3D scanning was performed using the FMT 4000 system with laser excitation at 680 nm for the detection of iRFP. TrueQuant software (version 3.0, PerkinElmer) was used to reconstruct the detected fluorescence signals. The regions of interest in the brain were manually circled for the quantification of fluorescence signals, and the resulting quantification data were expressed as the picomolar levels of iRFP.

Survival assay using intracerebral glioma models

Intracerebral U87-iRFP gliomas were established by stereotactic injection into the right frontal lobe in nude mice as described above. Seven days later, the mice were stereotactically injected with 2×10^5 hASC-ACE-CDs (n = 18) or 1×10^4 TUs of ACE-CD vector (n = 12) at the tumor implantation site. Five weeks later, nine hASC-ACE-CD-treated and six ACE-CD-treated mice received daily intraperitoneal injections of 5-FC (500 mg/kg), while the remaining nine hASC-ACE-CD-treated and six ACE-CD-treated mice received daily intraperitoneal injections of PBS for 7 consecutive days. This 7-day cycle of 5-FC or PBS administration was repeated every 1 or 2 weeks.

Genomic DNA extraction

Genomic DNA was extracted from mouse tissue samples using a Tissue DNA Isolation Kit (Geneaid, Taipei, Taiwan). The extracted DNA was quantified and stored at -20 °C until further use.

Real-time PCR analysis

To detect any integrated RRV sequence in tissue genome, real-time PCR was performed as described previously [39] using an ABI StepOne real-time PCR system (Applied Biosystems). A pair of primers specifically targeting the 4070A amphotropic *env* were used: forward primer 5′-ACCCTCAACCTCCCCTACAAG-3′ and reverse primer 5′-GTTAAGCGCCTGATAGGCTC-3′. Copy number of apolipoprotein B was also quantified as an internal control to ensure precise amounts of input genomic DNA (forward primer 5′-CACGTGGGCTCCAGCATT-3′; reverse primer 5′-TCACCAGTCATTTCTGCCTTTG-3′).

Statistical analysis

The t-test was used to compare *in vitro* cytotoxicity, cell migration, and *in vivo* viral replication between two independent groups. One-way ANOVA was conducted for the comparison of iRFP fluorescence intensities among multiple groups. Kaplan-Meier analysis and log-rank tests were used to evaluate survival. All analyses were conducted using SAS version 9.4 (SAS Institute).

RESULTS

hASCs are permissive to RRV infection and become RRV producer cells

To assess the ability of RRVs to transduce and replicate in hASCs, we infected hASCs with ACE-GFP vector (**Fig. 1A**) at an MOI of 0.2. Flow cytometry confirmed that ACE-GFP could replicate in hASCs, achieving >95% transduction (**Fig. 1B**). To evaluate the ability of hASC-ACE-GFPs to transmit the viral vector to glioma cells, conditioned media harvested from the hASC-ACE-GFP culture was applied to U87 glioma cells, and the transduction of U87 cells was subsequently monitored based on the GFP expression. The viral vector released from hASC-ACE-GFPs exhibited robust replication in U87 cells, with approximately 95% of U87 cells expressing GFP within 6 days (**Fig. 1C**). These results indicate that hASCs are highly permissive to RRV infection and could serve as effective producer cells of RRVs. We further investigated the replication kinetics of ACE-GFP in U87 cells by initially mixing hASC-ACE-GFPs and U87-dsRed cells at various percentages. When even as few as 0.01% of the mixed cell population comprised ACE-GFP-producing hASCs, nearly the entire cell population exhibited both GFP and dsRed fluorescence by day 9 (**Fig. 1D**), with the replication kinetics being more rapid when the percentage of initial ACE-GFP-producing hASCs was higher.

hASCs exhibit tumor-tropic migration toward glioma cells *in vitro*

The tumor-tropic migratory property of hASCs was evaluated by performing a Transwell migration assay in which hASCs were allowed to migrate toward U87 and SVGA cells or FBS alone. Both U87 and SVGA cells induced hASC migration, whereas few cells migrated toward the low-serum (0.5% FBS) control (**Fig. 2A**). Among the three tested conditions, U87 cells in the low-serum control induced the largest number of migrating hASCs, significantly exceeding the number of migrating hASCs induced by the high-serum (10% FBS) positive control and SVGA cells in the low-serum control (**Fig. 2B**). The results indicate that hASCs exhibit preferential migration toward glioma cells *in vitro*, supporting their potential utility as tumor-targeting delivery vehicles in glioma therapy.

Efficient hASC-mediated delivery of RRVs to gliomas *in vivo*

We evaluated the ability of hASCs to efficiently deliver RRVs in tumors *in vivo* by

testing hASC-ACE-GFPs in an intracerebral U87 glioma model. hASC-ACE-GFPs were injected into either the U87-dsRed tumor implantation site or the contralateral frontal lobe in nude mice bearing U87-dsRed glioma. Flow cytometry of dissected tumors revealed that 88.6±4.1% (mean±standard deviation) of tumors contained GFP and dsRed double-positive cells when hASC-ACE-GFPs were injected into the tumor implantation site, indicating the highly efficient hASC-mediated delivery of RRVs to gliomas (**Fig. 3A**). When hASC-ACE-GFPs were injected into the contralateral frontal lobe, 40.5±25.1% of tumors contained GFP and dsRed double-positive cells, demonstrating that hASC-ACE-GFPs were able to migrate from the contralateral site to the tumor and transfer RRVs to transduce tumor cells, albeit with greater variability. These results were also confirmed by fluorescence microscopy of brain cryosections showing the colocalization of GFP and dsRed signals in tumor cells (**Fig. 3B**).

hASC-ACE-CDs exert a potent killing effect against glioma cells after prodrug administration

The therapeutic potential of the hASC delivery platform was assessed by incubating 5-FC with hASC-ACE-CDs mixed with uninfected U87 cells (**Fig. 1A**). Substantial cell killing was observed after incubation with 5-FC even when only 10% of the mixed cell population produced ACE-CD (**Fig. 4A**), indicating an increase in the ACE-CD-transduced population by the replicative spread of ACE-CD vector released from hASC-ACE-CDs. The self-clearance capability of hASC-ACE-CDs was assessed by examining the susceptibility to 5-FC-induced cell death. The cell viability decreased to 68.0% and 26.4% after 4 and 8 days of 5-FC treatment, respectively, with nearly all cells cleared by day 16 (**Fig. 4B**). These findings indicate that hASC-ACE-CDs are susceptible to 5-FU produced from the CD-mediated conversion of 5-FC, thereby strongly facilitating their clearance from the brain after being intracranially injected, which reduces safety concerns about long-term stem-cell persistence.

hASC-mediated RRV delivery significantly suppresses tumor growth and improves survival

To evaluate and compare the *in vivo* therapeutic efficacy of hASC-mediated RRV delivery and direct injection of RRVs alone, hASC-ACE-CDs or ACE-CD vectors

were injected into the tumor implantation site in mice bearing intracerebral gliomas, followed by the systemic administration of 5-FC. FMT imaging of the mice showed changes in intracranial iRFP fluorescence signals over time in the hASC-ACE-CD/PBS control group and the hASC-ACE-CD/5-FC treatment group, and revealed significant tumor suppression in the latter group (**Fig. 5A**). The intracranial iRFP fluorescence signals were markedly lower in the hASC-ACE-CD/5-FC group than in the ACE-CD/5-FC group (**Fig. 5B**). Notably, while both the hASC-ACE-CD/5-FC and ACE-CD/5-FC groups showed prolonged survival (**Fig. 6**), tumor suppression and survival were sustained for longer in the former group, suggesting that the therapeutic benefit was greater for hASC-mediated RRV delivery.

No detectable dissemination of RRVs to extratumoral organs

The biosafety of this therapeutic strategy was assessed by conducting quantitative real-time PCRs of genomic DNA isolated from tumors and various extratumoral organs including lung, liver, spleen, intestine, heart, and brain, using primers specific for the 4070A amphotropic *env* (**Table 1**). As expected, the 4070A amphotropic *env* sequence could be readily detected in hASC-ACE-CD-injected tumor tissues, while no detectable dissemination was observed in any of the extratumoral organs obtained from the same animals.

DISCUSSION

MSCs have been referred to as a double-edged sword in tumor growth due to their roles in both promoting and suppressing tumor progression [40]. Their self-renewal capacity, *in vitro* expansion potential, and preferential migration to tumor sites make them ideal candidates as vehicles for delivering therapeutic molecules to cancers [41]. While the risks of using MSCs in cancer therapies are acknowledged, the potential benefits remain compelling [42]. The present study exploited hASCs as vehicles to effectively deliver RRVs for use in glioma gene therapy, with the results showing that hASCs actively migrated toward glioma cells *in vitro* and toward glioma xenografts to deliver RRVs *in vivo*. This capability may be particularly valuable for targeting residual tumors or infiltrative tumor cells distant from tumor resection sites, which are especially challenging to eliminate.

The *in vivo* experiments performed in this study showed that survival was significantly prolonged in both the hASC-ACE-CD/5-FC and ACE-CD/5-FC treatment groups. Notably, the hASC-ACE-CD/5-FC group demonstrated a superior survival benefit, accompanied by long-term tumor suppression as confirmed by FMT imaging. This concordance between reduced tumor size and prolonged survival underscores the superior therapeutic effects of hASC-mediated RRV delivery. Despite inter-animal variability, the consistently stronger and sustained tumor suppression in the hASC-ACE-CD/5-FC group highlights the robustness of this strategy.

For future treatment regimens, we propose that hASC-ACE-CDs could be used to target residual tumor cells in GBM patients by administering the cells to postresection tumor cavity margins followed by 5-FC treatments. Compared with the direct injection of ACE-CD vectors, hASC-mediated RRV delivery has been demonstrated to achieve greater and more-rapid RRV penetration by migrating through the tumor mass and into tumor foci infiltrating normal brain tissue. Furthermore, hASC-ACE-CDs exhibited a self-elimination feature by mediating the conversion of 5-FC to 5-FU, effectively undergoing cell death alongside glioma cells. This built-in “suicide switch” provides a self-limiting mechanism that increases safety by minimizing long-term stem-cell persistence or the potential transformation risk of MSCs. Such a design represents a significant improvement in the safety profile of cell-based gene therapies.

The present real-time PCR analyses demonstrated that the distribution of RRVs

delivered by hASCs is highly restricted to the tumor itself, with no spread to extratumoral organs. This result is consistent with our previous study showing that RRVs delivered to intracerebral RG-2 tumors in an immune-competent glioma model showed no detectable spread to all of the normal tissues examined [8]. Accordingly, clinical trials (NCT01470794 and NCT02414165) using the RRVs encoding the CD gene in patients with recurrent high-grade gliomas have found no adverse effects related to malignant transformation [10, 11]. Notwithstanding the promising findings of this study, the clinical development of hASC-mediated RRV delivery platforms will require further confirmation of their safety, biodistribution, and therapeutic efficacy. This study has highlighted the dual function of hASCs as both effective RRV producers and glioma-targeting vehicles, offering a promising platform for safe and effective gene therapy against glioma.

Figure Legends

Fig. 1. Structure of replicating retroviral vectors (RRVs) and their infection of human adipose-derived stem cells (hASCs) and U87 glioma cells.

(A) Schematic representation of the RRVs constructs carrying transgenes. The vectors contain an internal ribosome entry site (IRES) followed by green fluorescent protein (GFP) or cytosine deaminase (CD), positioned between *env* and 3′-UTR. ψ denotes the packaging signal. **(B)** hASCs were inoculated with ACE-GFP at an MOI of 0.2, and flow cytometry was used to assess the transduction of hASCs by ACE-GFP. **(C)** Replication of ACE-GFP in U87 cells exposed to conditioned medium collected from the hASC-ACE-GFP culture. Flow cytometry was used to analyze U87 cells for the expression of GFP over time. **(D)** hASC-ACE-GFPs were mixed with U87-dsRed cells at 0.01%, 0.1%, and 1% of the cell population and seeded onto six-well plates. The cell populations were analyzed at various time points postinfection for the expressions of GFP and dsRed.

Fig. 2. Migration of hASCs assessed using the Transwell assay.

(A) Representative images showing the migration of hASCs in response to different chemoattractants placed in the lower chamber: 0.5% FBS, 10% FBS, U87 cells with 0.5% FBS, and SVGA cells with 0.5% FBS. **(B)** Quantitative analysis of hASCs that migrated across the Transwell membrane under each condition. Data are mean±standard-deviation values. $*P < 0.01$.

Fig. 3. Efficient hASC-mediated delivery of RRVs to gliomas *in vivo*.

Intracerebral gliomas were established by injecting U87-dsRed cells into the right frontal lobe of BALB/c nude mice. Tumor-bearing mice were injected with hASC-ACE-GFPs at the tumor implantation site or at the contralateral frontal lobe. **(A)** Tumors were excised 4 weeks later, and flow cytometry was used to determine the expression levels of GFP and dsRed in dissociated tumor cells. The percentages of GFP and dsRed double-positive cells in tumors are indicated. X-axis (FL1): GFP fluorescence; Y-axis (FL2): dsRed fluorescence. **(B)** Representative fluorescence microscopy images of cryosectioned brains showing the colocalization of GFP and dsRed fluorescence in tumor cells. H&E, hematoxylin and eosin staining. Merged,

merged dsRed and GFP images. T, tumor. N, normal brain.

Fig. 4. *In vitro* cytotoxicity achieved by hASC-ACE-CDs followed by 5-FC administration.

(A) hASCs, hASC-ACE-GFPs, and hASC-ACE-CDs were mixed with U87 cells at 10% of the cell population and seeded onto replicate 96-well plates. After overnight culture, the mixed cell populations were exposed to 0.5 mM 5-FC, and cell viability was determined 4 and 8 days later using the MTS assay. **(B)** Self-clearance of hASC-ACE-CDs after 5-FC treatment. Cell viability was determined using the MTS assay at different times after treatment with 0.5 mM 5-FC. Experiments were performed in triplicate. Data are mean±standard-deviation values. *$P < 0.05$, **$P < 0.001$.

Fig. 5. Fluorescence molecular tomography (FMT) imaging of the size of intracerebral gliomas.

FMT imaging of mice treated with hASC-ACE-CDs plus PBS, hASC-ACE-CDs plus 5-FC, ACE-CD plus PBS, or ACE-CD plus 5-FC. **(A)** Representative FMT images showing changes in the intracranial iRFP fluorescence signals over time in the hASC-ACE-CD/PBS and hASC-ACE-CD/5-FC groups. **(B)** iRFP fluorescence signals were measured weekly and expressed as the picomolar levels of iRFP. Solid lines represent the mean iRFP fluorescence intensities, and shaded areas indicate the corresponding standard deviations. Arrows indicate the times of 5-FC dosing. *P(hASC-ACE-CD/5-FC vs ACE-CD/5-FC) < 0.01, **P(hASC-ACE-CD/5-FC vs ACE-CD/5-FC) < 0.001.

Fig. 6. Survival of mice bearing intracerebral gliomas.

Overall survival times of mice treated with hASC-ACE-CDs plus PBS, hASC-ACE-CDs plus 5-FC, ACE-CD plus PBS, or ACE-CD plus 5-FC. Log-rank (Kaplan-Meier) tests were used to evaluate survival: P(hASC-ACE-CD/PBS vs hASC-ACE-CD/5-FC) = 1.0×10^{-5}, P(ACE-CD/PBS vs ACE-CD/5-FC) = 1.7×10^{-3}, and P(hASC-ACE-CD/5-FC vs ACE-CD/5-FC) = 0.021.

Table 1. Biodistribution of the RRVs after intratumoral injection of hASC-ACE-CDs in an intracerebral glioma model.

	Copies of 4070A amphotropic *env* per cell
Lung	–
Liver	–
Spleen	–
Intestine	–
Heart	–
Contralateral normal brain	–
Tumor	4.45±0.74

Genomic DNA extracted from lung, liver, spleen, intestine, heart, brain and intracerebral tumor of hASC-ACE-CD-injected mice was examined by real-time PCR assay. The numbers of 4070A amphotropic *env* copies per cell are presented as mean±standard deviation. –, not detectable (detection limit was 0.001 copy per cell).

ACKNOWLEDGEMENTS

We thank Dr Noriyuki Kasahara at UCSF for many helpful suggestions and discussion.

AUTHOR CONTRIBUTIONS

S-WL performed the laboratory experiments and drafted the manuscript. Y-TC contributed in the laboratory works. J-MS analyzed and interpreted the results of the experiments. P-CK performed data analyses. Y-HC and C-KT conceived and coordinated the overall study and revised the manuscript. All authors have read and agreed to the published version of the manuscript.

FUNDING

This study was supported by Ditmanson Medical Foundation Chia-Yi Christian Hospital Research Program (R109-36), Ditmanson Medical Foundation Chia-Yi Christian Hospital–National Chung Cheng University Joint Research Program (CYCH-CCU-2025-01) and Chang Gung Memorial Hospital (CMRPG6H0623).

COMPETING INTERESTS

The authors declare no competing interests.

ETHICAL APPROVAL

All animal experiments were conducted in accordance with the approval of the Institutional Animal Care and Use Committee at National Chung Cheng University, Taiwan (IACUC no. 1070201).

ADDITIONAL INFORMATION

Correspondence and requests for materials should be addressed to Yu-Hao Chen or Chien-Kuo Tai.

References

1. Louis DN, Perry A, Reifenberger G, von Deimling A, Figarella-Branger D, Cavenee WK, et al. The 2016 World Health Organization Classification of Tumors of the Central Nervous System: a summary. Acta Neuropathol. 2016;131:803-20.
2. D'Alessio A, Proietti G, Sica G, Scicchitano BM. Pathological and Molecular Features of Glioblastoma and Its Peritumoral Tissue. Cancers (Basel). 2019;11.
3. Agnihotri S, Burrell KE, Wolf A, Jalali S, Hawkins C, Rutka JT, et al. Glioblastoma, a brief review of history, molecular genetics, animal models and novel therapeutic strategies. Arch Immunol Ther Exp (Warsz). 2013;61:25-41.
4. Rainov NG. A phase III clinical evaluation of herpes simplex virus type 1 thymidine kinase and ganciclovir gene therapy as an adjuvant to surgical resection and radiation in adults with previously untreated glioblastoma multiforme. Hum Gene Ther. 2000;11:2389-401.
5. Tai CK, Wang W, Lai YH, Logg CR, Parker WB, Li YF, et al. Enhanced efficiency of prodrug activation therapy by tumor-selective replicating retrovirus vectors armed with the Escherichia coli purine nucleoside phosphorylase gene. Cancer Gene Ther. 2010;17:614-23.
6. Tai CK, Wang WJ, Chen TC, Kasahara N. Single-shot, multicycle suicide gene therapy by replication-competent retrovirus vectors achieves long-term survival benefit in experimental glioma. Mol Ther. 2005;12:842-51.
7. Huang TT, Parab S, Burnett R, Diago O, Ostertag D, Hofman FM, et al. Intravenous administration of retroviral replicating vector, Toca 511, demonstrates therapeutic efficacy in orthotopic immune-competent mouse glioma model. Hum Gene Ther. 2015;26:82-93.
8. Wang W, Tai CK, Kershaw AD, Solly SK, Klatzmann D, Kasahara N, et al. Use of replication-competent retroviral vectors in an immunocompetent intracranial glioma model. Neurosurg Focus. 2006;20:E25.
9. Chen SH, Sun JM, Chen BM, Lin SC, Chang HF, Collins S, et al. Efficient Prodrug Activator Gene Therapy by Retroviral Replicating Vectors Prolongs Survival in an Immune-Competent Intracerebral Glioma Model. Int J Mol Sci. 2020;21.
10. Cloughesy TF, Landolfi J, Vogelbaum MA, Ostertag D, Elder JB, Bloomfield S, et al. Durable complete responses in some recurrent high-grade glioma patients

treated with Toca 511 + Toca FC. Neuro Oncol. 2018;20:1383-92.

11. Cloughesy TF, Petrecca K, Walbert T, Butowski N, Salacz M, Perry J, et al. Effect of Vocimagene Amiretrorepvec in Combination With Flucytosine vs Standard of Care on Survival Following Tumor Resection in Patients With Recurrent High-Grade Glioma: A Randomized Clinical Trial. JAMA Oncol. 2020;6:1939-46.

12. Hmadcha A, Martin-Montalvo A, Gauthier BR, Soria B, Capilla-Gonzalez V. Therapeutic Potential of Mesenchymal Stem Cells for Cancer Therapy. Front Bioeng Biotechnol. 2020;8:43.

13. Xie C, Yang Z, Suo Y, Chen Q, Wei D, Weng X, et al. Systemically Infused Mesenchymal Stem Cells Show Different Homing Profiles in Healthy and Tumor Mouse Models. Stem Cells Transl Med. 2017;6:1120-31.

14. Smith CL, Chaichana KL, Lee YM, Lin B, Stanko KM, O'Donnell T, et al. Pre-exposure of human adipose mesenchymal stem cells to soluble factors enhances their homing to brain cancer. Stem Cells Transl Med. 2015;4:239-51.

15. Kidd S, Spaeth E, Dembinski JL, Dietrich M, Watson K, Klopp A, et al. Direct evidence of mesenchymal stem cell tropism for tumor and wounding microenvironments using in vivo bioluminescent imaging. Stem Cells. 2009;27:2614-23.

16. Spano C, Grisendi G, Golinelli G, Rossignoli F, Prapa M, Bestagno M, et al. Soluble TRAIL Armed Human MSC As Gene Therapy For Pancreatic Cancer. Sci Rep. 2019;9:1788.

17. Marofi F, Vahedi G, Biglari A, Esmaeilzadeh A, Athari SS. Mesenchymal Stromal/Stem Cells: A New Era in the Cell-Based Targeted Gene Therapy of Cancer. Front Immunol. 2017;8:1770.

18. Xu G, Guo Y, Seng Z, Cui G, Qu J. Bone marrow-derived mesenchymal stem cells co-expressing interleukin-18 and interferon-beta exhibit potent antitumor effect against intracranial glioma in rats. Oncol Rep. 2015;34:1915-22.

19. Yang X, Du J, Xu X, Xu C, Song W. IFN-gamma-secreting-mesenchymal stem cells exert an antitumor effect in vivo via the TRAIL pathway. J Immunol Res. 2014;2014:318098.

20. Seo SH, Kim KS, Park SH, Suh YS, Kim SJ, Jeun SS, et al. The effects of mesenchymal stem cells injected via different routes on modified IL-12-mediated antitumor activity. Gene Ther. 2011;18:488-95.

21. Kidd S, Caldwell L, Dietrich M, Samudio I, Spaeth EL, Watson K, et al. Mesenchymal stromal cells alone or expressing interferon-beta suppress pancreatic tumors in vivo, an effect countered by anti-inflammatory treatment. Cytotherapy. 2010;12:615-25.

22. Xin H, Sun R, Kanehira M, Takahata T, Itoh J, Mizuguchi H, et al. Intratracheal delivery of CX3CL1-expressing mesenchymal stem cells to multiple lung tumors. Mol Med. 2009;15:321-7.

23. Ren C, Kumar S, Chanda D, Chen J, Mountz JD, Ponnazhagan S. Therapeutic potential of mesenchymal stem cells producing interferon-alpha in a mouse melanoma lung metastasis model. Stem Cells. 2008;26:2332-8.

24. Aboody KS, Najbauer J, Danks MK. Stem and progenitor cell-mediated tumor selective gene therapy. Gene Ther. 2008;15:739-52.

25. Nakamizo A, Marini F, Amano T, Khan A, Studeny M, Gumin J, et al. Human bone marrow-derived mesenchymal stem cells in the treatment of gliomas. Cancer Res. 2005;65:3307-18.

26. Oraee-Yazdani S, Tavanaei R, Rostami F, Hajarizadeh A, Mehrabadi M, Akhlaghpasand M, et al. Suicide gene therapy using allogeneic adipose tissue-derived mesenchymal stem cell gene delivery vehicles in recurrent glioblastoma multiforme: a first-in-human, dose-escalation, phase I clinical trial. J Transl Med. 2023;21:350.

27. Yoo KH, Jang IK, Lee MW, Kim HE, Yang MS, Eom Y, et al. Comparison of immunomodulatory properties of mesenchymal stem cells derived from adult human tissues. Cell Immunol. 2009;259:150-6.

28. Locke M, Feisst V, Dunbar PR. Concise review: human adipose-derived stem cells: separating promise from clinical need. Stem Cells. 2011;29:404-11.

29. Pendleton C, Li Q, Chesler DA, Yuan K, Guerrero-Cazares H, Quinones-Hinojosa A. Mesenchymal stem cells derived from adipose tissue vs bone marrow: in vitro comparison of their tropism towards gliomas. PLoS One. 2013;8:e58198.

30. Ceccarelli S, Pontecorvi P, Anastasiadou E, Napoli C, Marchese C. Immunomodulatory Effect of Adipose-Derived Stem Cells: The Cutting Edge of Clinical Application. Front Cell Dev Biol. 2020;8:236.

31. Choi SA, Hwang SK, Wang KC, Cho BK, Phi JH, Lee JY, et al. Therapeutic efficacy and safety of TRAIL-producing human adipose tissue-derived mesenchymal stem cells against experimental brainstem glioma. Neuro Oncol. 2011;13:61-9.

32. Choi SA, Lee JY, Wang KC, Phi JH, Song SH, Song J, et al. Human adipose tissue-derived mesenchymal stem cells: characteristics and therapeutic potential as cellular vehicles for prodrug gene therapy against brainstem gliomas. Eur J Cancer. 2012;48:129-37.
33. Jiang X, Fitch S, Wang C, Wilson C, Li J, Grant GA, et al. Nanoparticle engineered TRAIL-overexpressing adipose-derived stem cells target and eradicate glioblastoma via intracranial delivery. Proc Natl Acad Sci U S A. 2016;113:13857-62.
34. Huang WC, Lu IL, Chiang WH, Lin YW, Tsai YC, Chen HH, et al. Tumortropic adipose-derived stem cells carrying smart nanotherapeutics for targeted delivery and dual-modality therapy of orthotopic glioblastoma. Journal of Controlled Release. 2017;254:119-30.
35. Huang SP, Hsu CC, Chang SC, Wang CH, Deng SC, Dai NT, et al. Adipose-derived stem cells seeded on acellular dermal matrix grafts enhance wound healing in a murine model of a full-thickness defect. Ann Plast Surg. 2012;69:656-62.
36. Lu YC, Chen YJ, Yu YR, Lai YH, Cheng JC, Li YF, et al. Replicating retroviral vectors for oncolytic virotherapy of experimental hepatocellular carcinoma. Oncol Rep. 2012;28:21-6.
37. Chao CN, Yang YH, Wu MS, Chou MC, Fang CY, Lin MC, et al. Gene therapy for human glioblastoma using neurotropic JC virus-like particles as a gene delivery vector. Sci Rep. 2018;8:2213.
38. Chou CC, Tseng CE, Lin YS, Wang M, Chen PL, Chang D, et al. Inhibition of orthotopic castration-resistant prostate cancer growth and metastasis in mice by JC VLPs carrying a suicide gene driven by the PSA promoter. Cancer Gene Ther. 2024;31:250-8.
39. Lu YC, Luo YP, Wang YW, Tai CK. Highly efficient gene transfer to solid tumors in vivo by tumor-selective replicating retrovirus vectors. Int J Mol Med. 2010;25:769-75.
40. Liang W, Chen X, Zhang S, Fang J, Chen M, Xu Y, et al. Mesenchymal stem cells as a double-edged sword in tumor growth: focusing on MSC-derived cytokines. Cell Mol Biol Lett. 2021;26:3.
41. Lan T, Luo M, Wei X. Mesenchymal stem/stromal cells in cancer therapy. J Hematol Oncol. 2021;14:195.
42. Baran Z, Cetinkaya M, Baran Y. Mesenchymal Stem Cells in Cancer Therapy.

Adv Exp Med Biol. 2025;1474:149-77.

Figure 1

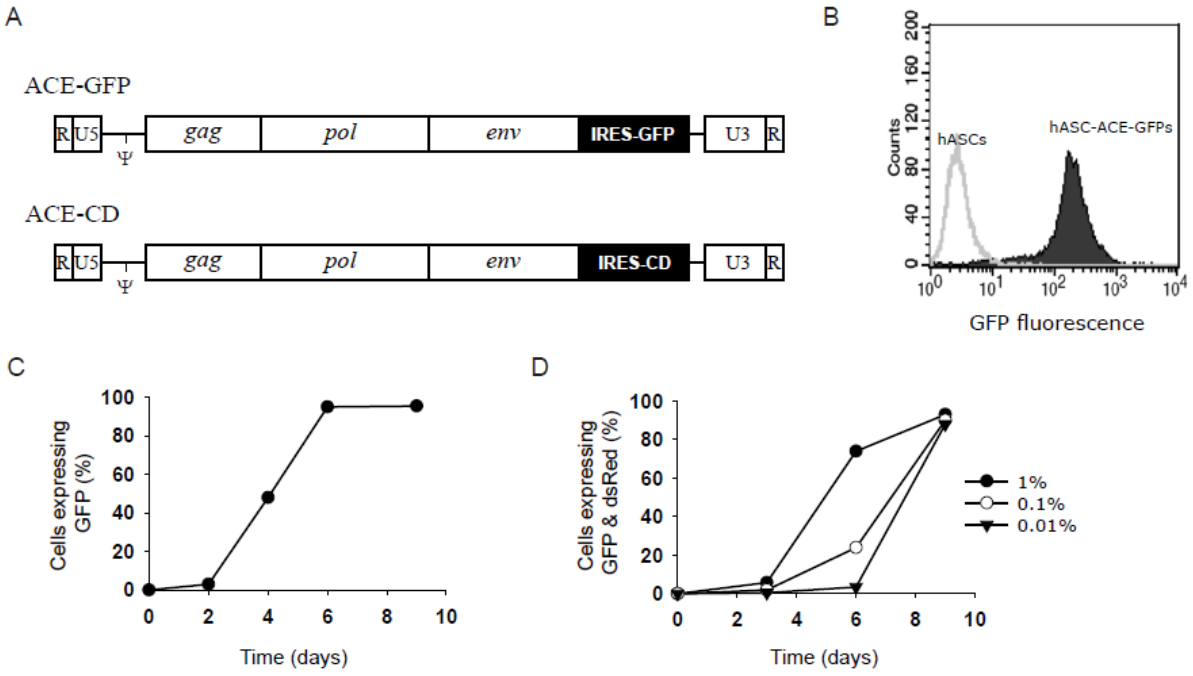

A
ACE-GFP
R
U5
Ψ
gag
pol
env
IRES-GFP
U3
R
ACE-CD
R
U5
Ψ
gag
pol
env
IRES-CD
U3
R
B
Counts
hASCs
hASC-ACE-GFPs
GFP fluorescence
C
Cells expressing GFP (%)
Time (days)
D
Cells expressing GFP & dsRed (%)
1%
0.1%
0.01%
Time (days)

Figure 2

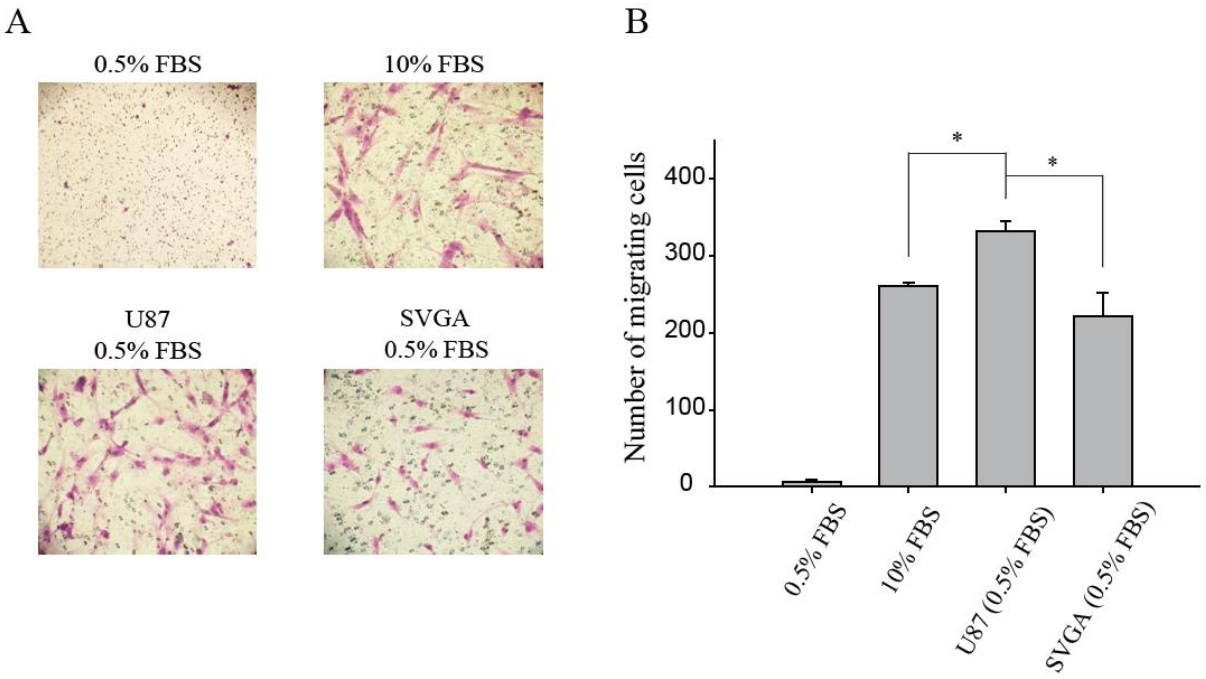

A
0.5% FBS
10% FBS
U87
0.5% FBS
SVGA
0.5% FBS
B
Number of migrating cells
400
300
200
100
0
*
*
0.5% FBS
10% FBS
U87 (0.5% FBS)
SVGA (0.5% FBS)

Figure 3

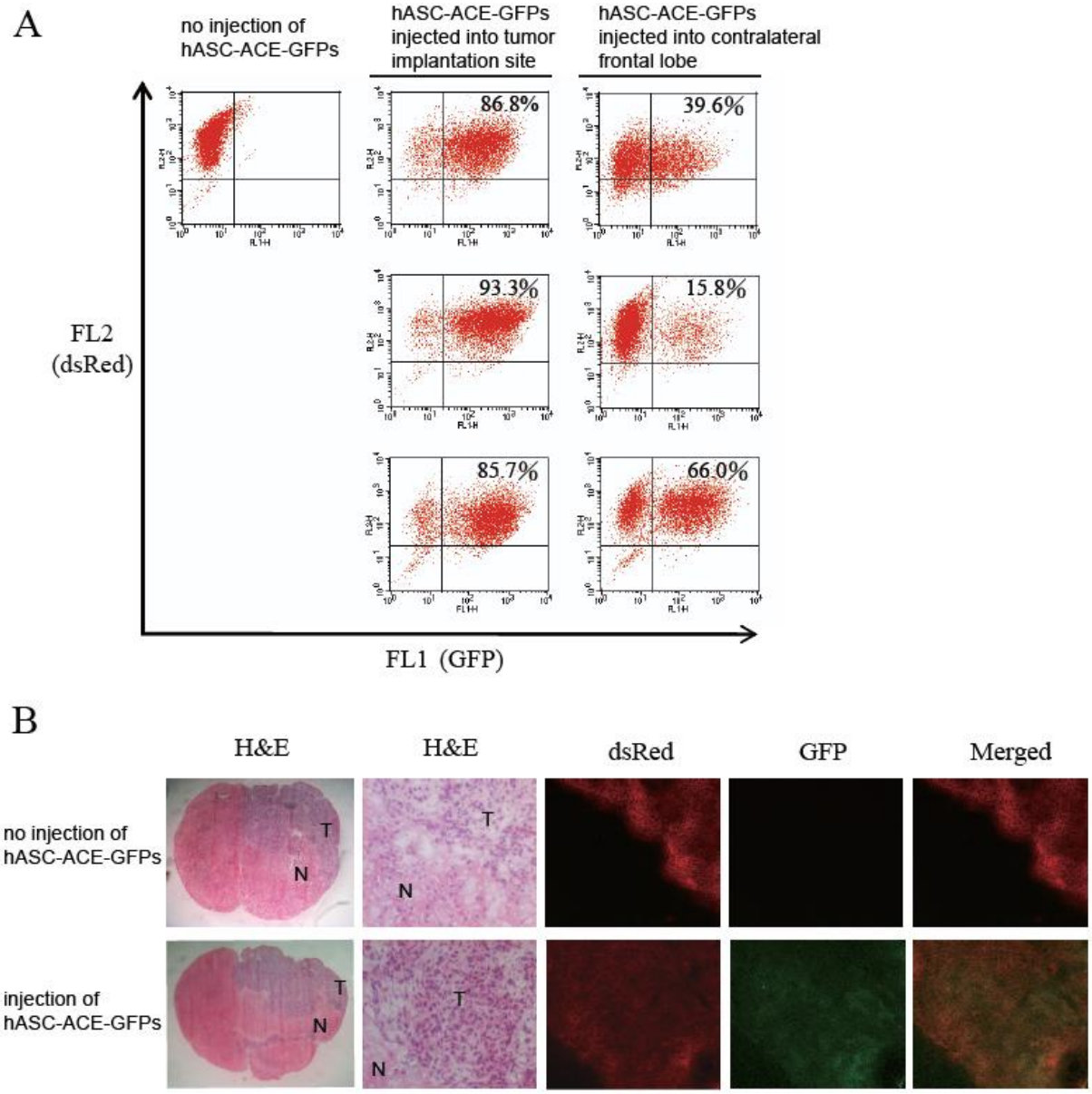

A
no injection of hASC-ACE-GFPs
hASC-ACE-GFPs injected into tumor implantation site
hASC-ACE-GFPs injected into contralateral frontal lobe
86.8%
39.6%
93.3%
15.8%
85.7%
66.0%
FL2 (dsRed)
FL1 (GFP)
B
H&E
H&E
dsRed
GFP
Merged
no injection of hASC-ACE-GFPs
injection of hASC-ACE-GFPs
T
N

Figure 4

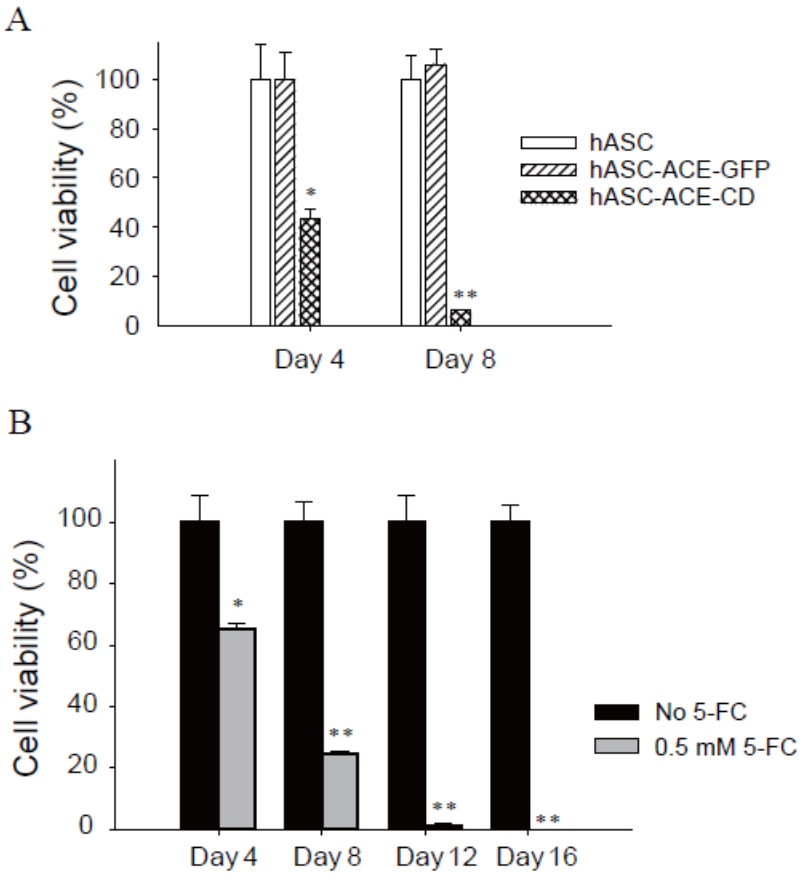
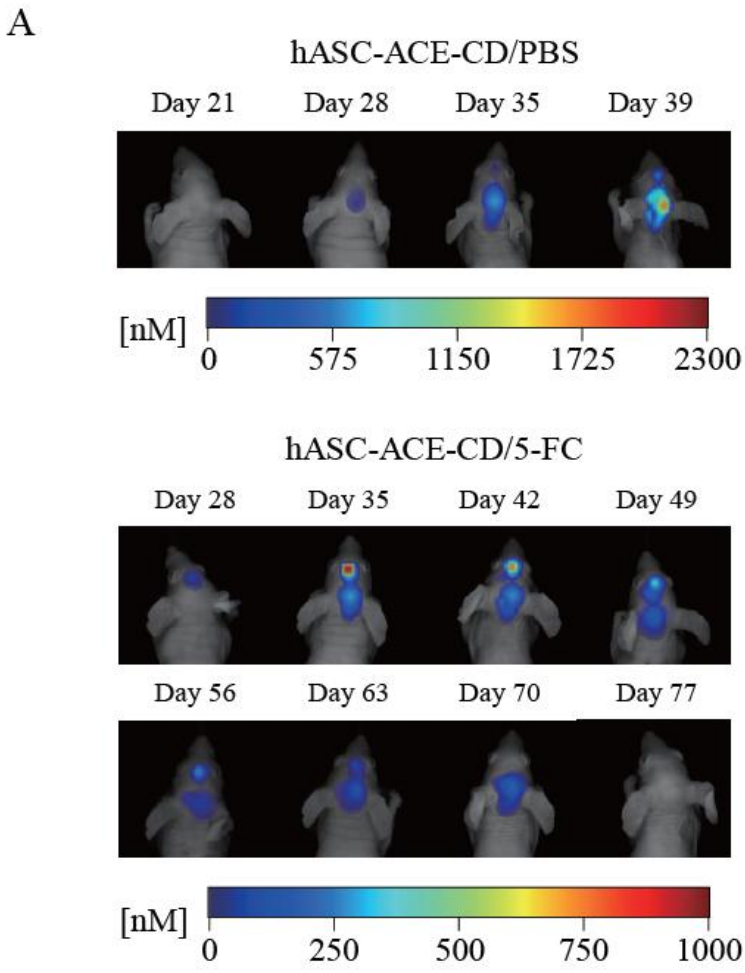

A
Cell viability (%)
100
80
60
40
20
0
*
**
Day 4
Day 8
hASC
hASC-ACE-GFP
hASC-ACE-CD
B
Cell viability (%)
100
80
60
40
20
0
*
**
**
**
Day 4
Day 8
Day 12
Day 16
No 5-FC
0.5 mM 5-FC

Figure 5


A
hASC-ACE-CD/PBS
Day 21
Day 28
Day 35
Day 39
[nM]
0
575
1150
1725
2300
hASC-ACE-CD/5-FC
Day 28
Day 35
Day 42
Day 49
Day 56
Day 63
Day 70
Day 77
[nM]
0
250
500
750
1000

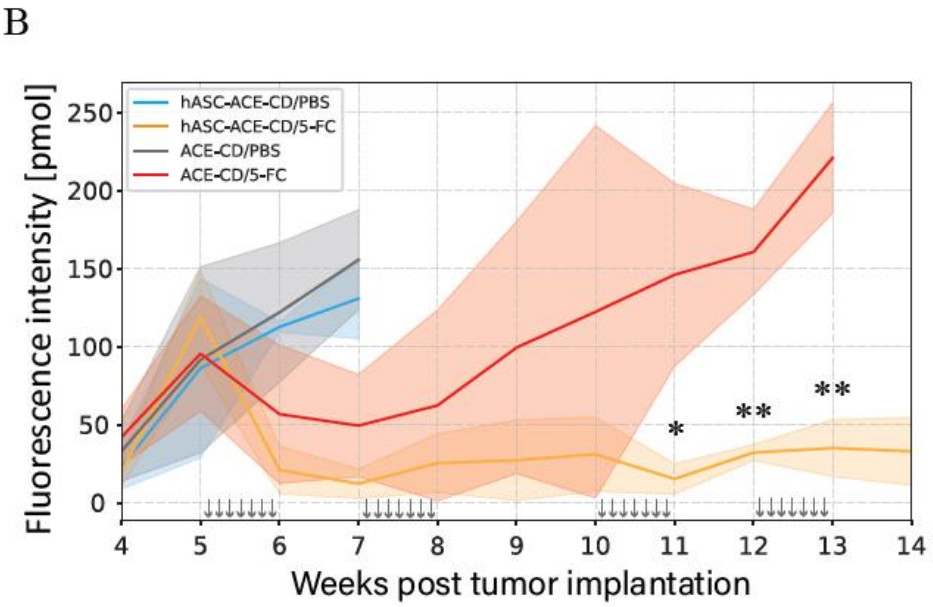
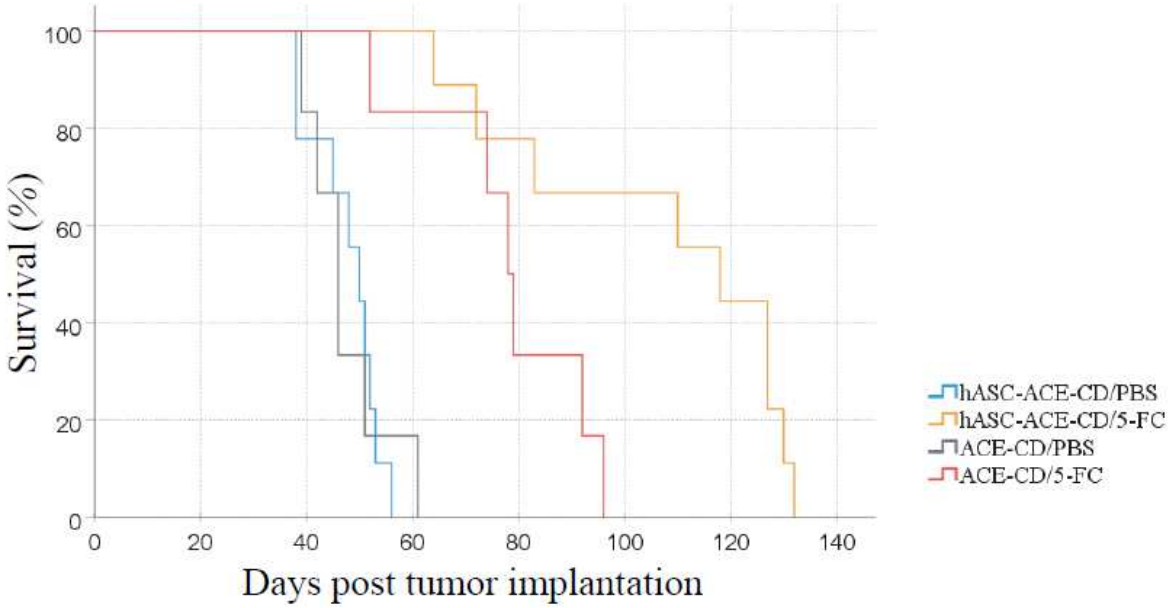

B
hASC-ACE-CD/PBS
hASC-ACE-CD/5-FC
ACE-CD/PBS
ACE-CD/5-FC
Fluorescence intensity [pmol]
250
200
150
100
50
0
*
**
**
4
5
6
7
8
9
10
11
12
13
14
Weeks post tumor implantation

Figure 6



Pairwise comparison	*P* value
hASC-ACE-CD/PBS vs hASC-ACE-CD/5-FC	1.0×10^{-5}
ACE-CD/PBS vs ACE-CD/5-FC	1.7×10^{-3}
hASC-ACE-CD/5-FC vs ACE-CD/5-FC	2.1×10^{-2}